SRTTU

Journal of Electrical and Computer Engineering Innovations

JECEI, Vol. 7, No. 1, 2019

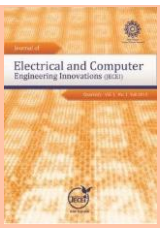

A Comprehensive Mathematical Model for Analysis of WR-Resolvers under Stator Short Circuit Fault

Hamed Lasjerdi[1], Zahra Nasiri-Gheidari[1,*], and Farid Tootoonchian[2]

[1]Department of Electrical Engineering, Sharif University of Technology, Tehran, Iran.

[2] Department of Electrical Engineering, Iran University of Science and Technology, Tehran, Iran.

[*]Corresponding Author's Information: znasiri@sharif.edu

The extended version of one of the ICEE2019's top papers.

ARTICLE INFO

ARTICLE HISTORY:
Received 26 June 2019
Revised 1 September 2019
Accepted 15 September 2019

KEYWORDS:
Wound Rotor (WR) resolver
Mathematical model
Short-Circuit (SC) fault
d-q axes

ABSTRACT

Wound-Rotor (WR) resolvers are the most widely used position sensors in applications with harsh environmental conditions. However, their performance is exposed to failure due to the high risk of short circuit (SC) fault. Although the output current of the resolver is negligible, its thin copper wires increase the probability of the short circuit fault. To avoid the propagation of the turn-to-turn SC fault to the whole coil and undesirable performance of the motion control drive, it is necessary to diagnose it at the very beginning of its development. Meanwhile, the first step of diagnosing faults is their modeling. Time stepping finite element analysis is the most accurate, but computationally expensive method for modeling the electromagnetic devices. Therefore, it is required to establish an accurate, yet computationally fast model. In this regard, an analytical model based on d-q axes theory is proposed to consider multiple faults, simultaneously. Then, the success of the proposed model is validated by experimental tests on the studied sensor.

1. INTRODUCTION

High-efficiency electrical machines are widely used in electric vehicles and other industrial applications [1]-[2]. Most of the high-efficiency machines are inverter-driven ones that their improved performance is depended on their accurate position estimation. In this regards, position sensors are employed. The most common position sensors are optical encoders and resolvers. Although optical encoders offer higher accuracy and lower cost, they have undesirable performance in harsh environments where there are wide temperature variation, high level of noise, and vibration [3]-[4]. Therefore, in such applications engineers prefer to use resolvers that have a robust structure due to their similarity to electrical machines. In fact, resolvers are two-phase synchronous generators with high-frequency excitation voltage. They have an excitation winding on the rotor and two-phase signal windings on the stator. Since the excitation winding is fed by an AC voltage, a rotary transformer (RT) can be used for non-contact transferring of the voltage [4]. In this regard, the primary coil of the RT is wound on a primary, stationary core of RT and fed using a high-frequency voltage. Then, the induced voltage on the secondary coil that is located on the rotor is used for supplying the rotor winding. Despite the advantages of RT in non-contact transferring the voltages, its usage adds some difficulties such as excessive dimensions of the sensor, increased phase-shift error, and accuracy deterioration as a result of RT's leakage flux linking the resolver's windings [5]. Therefore, some researches propose to omit the individual core of RT by grooving a new slot perpendicular to the main slots of the sensor [5]-[7].

Some other researchers try to omit the rotor winding and consequently their proposed resolvers

don't need any RT. They proposed variable reluctance (VR) resolvers [8]-[15]. VR resolvers have no-winding on the rotor and the excitation winding is moved to the stator side. They worked based on the sinusoidal variation of air-gap's reluctance. So, the resolvers are divided into two groups: sinusoidal air-gap length [8]-[10], and sinusoidal area [10]-[14] resolvers. Although VR resolvers have simpler structure and lower price in comparison to WR resolvers, they have some difficulties in 2-pole applications [15]. Therefore, in 2-pole applications, WR resolvers are often preferred to VR types and in the focus of this paper is on WR resolvers. Although there are different configurations of WR resolvers include cylindrical resolvers [16], disk type ones [3]-[8] and linear resolvers [17]-[18], the most commercial WR resolvers are cylindrical ones. Furthermore, none of the mentioned researches referred to electrical faults. However, there is high risk of short circuit fault in resolvers due to their thin wires. It worth noting that short circuit fault in other electrical machines is considered in literature [19]. However, the only manuscripts in this field are [20]-[23]. Among them [20]-[23] have been done on VR resolvers using finite element analysis. The only manuscript that discusses the short circuit fault of wound rotor resolvers is [23]. In [23] a mathematical model is proposed for performance evaluation of the WR resolvers under short circuit fault in stator windings. It is supposed that there is only one turn to turn fault in one of the stator windings. While in this paper that is the extended version of [23], the mathematical model and the equivalent circuit are obtained to consider multiple faults, simultaneously.

It should be mentioned that diagnosing turn-to-turn fault at the very beginning of its development is necessary to avoid the propagation of the turn-to-turn SC fault to the whole coil/winding(s) and undesirable performance of the motion control drive. In this regard, an accurate but computationally fast model is required. Although time stepping finite element method is the most reliable and accurate method for modeling of electromagnetic sensors, it is time-consuming and it is not recommended for use in on-line fault diagnosing/canceling programs. Therefore, in this paper, an analytical model based on d-q axes theory is proposed to study the performance of the WR resolvers. The success of the model is evaluated by experimental measurements.

2. Configuration of the Sensor

The studied resolver is a two-pole, cylindrical, WR resolver. Both the stator and the rotor have made from a laminated ferromagnetic material. The stator has 12 slots and the rotor has 16 slots. The schematic of the studied resolver's core along with its rotary transformer is shown in Fig. 1.

It should be mentioned that in WR resolvers usually a perpendicular winding is wound in the rotor slots along with the excitation winding. It is a short circuit winding, called damper winding [13]. For the healthy resolvers with conventional distributed or on-tooth variable turn windings, using the damper winding has no significant effect on the performance and only helps to improve the accuracy of the sensor under mechanical faults. While, for the resolvers equipped with the fractional slot or constant turn on-tooth winding, even in healthy condition using damper winding helps to suppress the sub-harmonics and improve the accuracy.

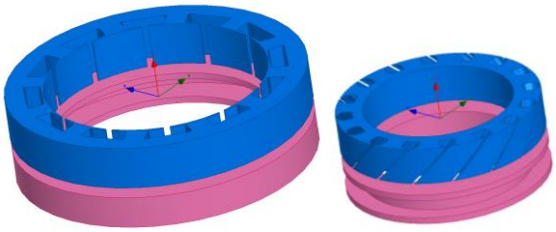

(a) (b)

Figure 1: The schematic of the studied brushless resolver: (a) The stator and the primary of RT, (b) The rotor and the secondary of RT.

3. Analytical Model

The schematic of the stator and rotor windings is shown in Fig. 2. As mentioned earlier, the stator has a two-phase perpendicular winding that is connected to the resolver to digital converter (RDC), called sine and cosine windings. Since the input impedance of the RDC is significantly high, the current in the signal windings of the resolver is negligible [4]. Also, the rotor has a two-phase perpendicular winding: the excitation winding that is fed by the secondary coil of RT and a damper winding. Some turn to turn short circuit faults are assumed on the stator windings, called SCA1, SCA2, …, SCAn, and SCB1, SCB2, …, SCBn .

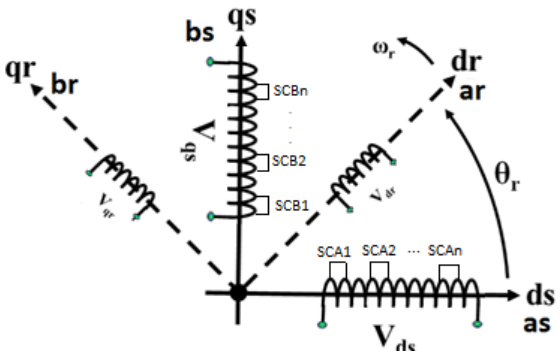

Figure 2: The schematic of the resolver's windings.

The voltage equations of the windings can be written as:

$$\begin{bmatrix} v_a^s \\ v_b^s \end{bmatrix} = \begin{bmatrix} R_s & 0 \\ 0 & R_s \end{bmatrix} \begin{bmatrix} i_a^s \\ i_b^s \end{bmatrix} + \frac{d}{dt} \begin{bmatrix} \lambda_a^s \\ \lambda_b^s \end{bmatrix} \quad (1)$$

$$\begin{bmatrix} v_a^r \\ v_b^r \end{bmatrix} = \begin{bmatrix} R_r & 0 \\ 0 & R_r \end{bmatrix} \begin{bmatrix} i_a^r \\ i_b^r \end{bmatrix} + \frac{d}{dt} \begin{bmatrix} \lambda_a^r \\ \lambda_b^r \end{bmatrix} \quad (2)$$

$$V_{scfk} = 0 = R_{scfk} i_{scfk} + \frac{d\lambda_{scfk}}{dt}, f = A, B \text{ and } k = 1 \text{ to } n \quad (3)$$

where R_s denotes the stator resistance, R_r rotor resistance, R_{scfk} short circuit turns' resistance, i current, v voltage, and λ flux linkage. Subscripts a, and b denotes phases a, and b, respectively. The superscripts s, r, and sc refer to stator, rotor, and short-circuit, respectively. The flux linkages, in the terms of the winding inductances and currents, for k=1, 2, …, n, can be written as:

$$\begin{bmatrix} \lambda_a^s \\ \lambda_b^s \end{bmatrix} = L_{ab}^{ss} \begin{bmatrix} i_a^s \\ i_b^s \end{bmatrix} + L_{ab}^{sr} \begin{bmatrix} i_a^r \\ i_b^r \end{bmatrix} + \sum_{k=1}^{n} \left(k_{scAk} L_{ms} \begin{bmatrix} I_{scAk} \\ 0 \end{bmatrix} + k_{scBk} L_{ms} \begin{bmatrix} 0 \\ I_{scBk} \end{bmatrix} \right) \quad (4)$$

$$\begin{bmatrix} \lambda_a^r \\ \lambda_b^r \end{bmatrix} = L_{ab}^{rs} \begin{bmatrix} i_a^s \\ i_b^s \end{bmatrix} + L_{ab}^{rr} \begin{bmatrix} i_a^r \\ i_b^r \end{bmatrix} + \sum_{k=1}^{n} \left(L^{rscAk} I_{scAk} + L^{rscBk} I_{scBk} \right) \quad (5)$$

$$\lambda_{scAk} = L^{scAks} \begin{bmatrix} i_a^s \\ i_b^s \end{bmatrix} + L^{scAkr} \begin{bmatrix} i_a^r \\ i_b^r \end{bmatrix} + \sum_{j=1}^{n} L^{scAkscAj} I_{scAj} \quad (6)$$

$$\lambda_{scBk} = L^{scBks} \begin{bmatrix} i_a^s \\ i_b^s \end{bmatrix} + L^{scBkr} \begin{bmatrix} i_a^r \\ i_b^r \end{bmatrix} + \sum_{j=1}^{n} L^{scBkscBj} I_{scBj} \quad (7)$$

where the submatrices of the stator-to-stator, and rotor-to-rotor, winding inductances are:

$$L_{ab}^{ss} = \begin{bmatrix} L_{asas} & L_{asbs} \\ L_{asbs} & L_{bsbs} \end{bmatrix} = \begin{bmatrix} L_{ls} + L_{ms} & 0 \\ 0 & L_{ls} + L_{ms} \end{bmatrix} \quad (8)$$

$$L_{ab}^{rr} = \begin{bmatrix} L_{arar} & L_{arbr} \\ L_{brar} & L_{brbr} \end{bmatrix} = \begin{bmatrix} L_{lr} + L_{mr} & 0 \\ 0 & L_{lr} + L_{mr} \end{bmatrix} \quad (9)$$

and those of mutual inductances, for k=1, 2, …, n, are defined as:

$$L_{ab}^{sr} = L_{sr} \begin{bmatrix} \cos\theta_r & -\sin\theta_r \\ \sin\theta_r & \cos\theta_r \end{bmatrix} \quad (10)$$

$$L^{scAkr} = L_{scAkr} [\cos(\theta_{scAk} - \theta_r) \quad \sin(\theta_{scAk} - \theta_r)] \quad (11)$$

$$L^{scBkr} = L_{scBkr} [\cos(\theta_{scBk} - \theta_r) \quad \sin(\theta_{scBk} - \theta_r)] \quad (12)$$

$$L^{scAks} = L_{scAks} [\cos(\theta_{scAk}) \quad \sin(\theta_{scAk})] \quad (13)$$

$$L^{scBks} = L_{scBks} [\cos(\theta_{scBk}) \quad \sin(\theta_{scBk})] \quad (14)$$

and for k, j=1 to n:

$$L^{scAkscAj} = \left(\frac{N_{scAk}}{N_s}\right)\left(\frac{N_{scAj}}{N_s}\right)(L_{ls} + L_{ms}) \cong (K_{scAk} \times K_{scAj}) L_{ms} \quad (15)$$

$$L^{scBkscBj} = \left(\frac{N_{scBk}}{N_s}\right)\left(\frac{N_{scBj}}{N_s}\right)(L_{ls} + L_{ms}) \cong (K_{scBk} \times K_{scBj}) L_{ms} \quad (16)$$

where L_{ls} is the per phase stator winding leakage inductance, L_{lr} is the per phase rotor winding leakage inductance, L_{ms} is the mutual inductance between the stator windings, L_{mr} is the mutual inductance between the rotor windings, L_{sr} is the peak value of the stator-to-rotor mutual inductance and L_{sckr}/L_{scks} are the value of the short circuit-to-rotor/stator mutual inductances. It should be mentioned that considering k=j in (15) and (16) gives the short turns-to-short turns winding inductances.

Neglecting MMF drops in ferromagnetic parts, the inductances can be re-written as:

$$L_{scAkr} = N_{scAk} N_r P_g = \frac{N_{scAk}}{N_s} N_s N_r P_g = k_{scAk} L_{sr} \quad (17)$$

$$L_{scBkr} = N_{scBk} N_r P_g = \frac{N_{scBk}}{N_s} N_s N_r P_g = k_{scBk} L_{sr} \quad (18)$$

$$L_{scAks} = N_{scAk} N_s P_g = \frac{N_{scAk}}{N_s} N_s N_s P_g = k_{scAk} L_{ms} \quad (19)$$

$$L_{scBks} = N_{scBk} N_s P_g = \frac{N_{scBk}}{N_s} N_s N_s P_g = k_{scBk} L_{ms} \quad (20)$$

Then, to facilitate the computation of the transient solution of the resolver, it is required to transfer the differential equations with time-varying inductances to differential equations with constant inductances. In this regards, d-q mathematical transformation is used. The transformation matrix and its invers are:

$$[T_{dq}] = \begin{bmatrix} cos\,\theta_r & -sin\theta_r \\ sin\theta_r & cos\,\theta_r \end{bmatrix} \quad (21)$$

$$[T_{dq}]^{-1} = \begin{bmatrix} cos\,\theta_r & sin\theta_r \\ -sin\theta_r & cos\,\theta_r \end{bmatrix} \quad (22)$$

Then, the equations can be written in stationary reference frame. Furthermore, the rotor and the short circuit quantities should be referred to the stator side. Finally, the stator and rotor voltage equations can be written as:

$$\begin{bmatrix} v_d^s \\ v_q^s \end{bmatrix} = R_s \begin{bmatrix} i_d^s \\ i_q^s \end{bmatrix} + \frac{d}{dt}\begin{bmatrix} \lambda_d^s \\ \lambda_q^s \end{bmatrix} \quad (23)$$

$$\begin{bmatrix} v_d'^r \\ v_q'^r \end{bmatrix} = \left(\frac{N_s}{N_r}\right)^2 R_r \begin{bmatrix} i_d'^r \\ i_q'^r \end{bmatrix} + \frac{d}{dt}\begin{bmatrix} \lambda_d'^r \\ \lambda_q'^r \end{bmatrix} + \omega \begin{bmatrix} 0 & 1 \\ -1 & 0 \end{bmatrix} \begin{bmatrix} \lambda_d'^r \\ \lambda_q'^r \end{bmatrix} \quad (24)$$

where

$$\begin{bmatrix} \lambda_d^s \\ \lambda_q^s \end{bmatrix} = L_{ls} \begin{bmatrix} i_d^s \\ i_q^s \end{bmatrix} + L_{ms}\left(\begin{bmatrix} i_d^s \\ i_q^s \end{bmatrix} + \begin{bmatrix} i_d'^r \\ i_q'^r \end{bmatrix} + \sum_{k=1}^{n} \left(\begin{bmatrix} I'_{scAk} \\ 0 \end{bmatrix} + \begin{bmatrix} 0 \\ I'_{scBk} \end{bmatrix}\right) = \begin{bmatrix} \lambda_d^{ls} \\ \lambda_q^{ls} \end{bmatrix} + \begin{bmatrix} \lambda_d^m \\ \lambda_q^m \end{bmatrix} \quad (25)$$

$$\begin{bmatrix} \lambda_d'^r \\ \lambda_q'^r \end{bmatrix} = \left(\left(\frac{N_s}{N_r}\right)^2 L_{lr}\right) \begin{bmatrix} i_d'^r \\ i_q'^r \end{bmatrix} + L_{ms}\left(\begin{bmatrix} i_d^s \\ i_q^s \end{bmatrix} + \begin{bmatrix} i_d'^r \\ i_q'^r \end{bmatrix} + \sum_{k=1}^{n} \left(\begin{bmatrix} I'_{scAk} \\ 0 \end{bmatrix} + \begin{bmatrix} 0 \\ I'_{scBk} \end{bmatrix}\right) = \begin{bmatrix} \lambda_d'^{lr} \\ \lambda_q'^{lr} \end{bmatrix} + \begin{bmatrix} \lambda_d^m \\ \lambda_q^m \end{bmatrix} \quad (26)$$

For the voltage equation of short-circuit winding, considering *f*=*A*, and *B*, and *k*=*1, 2*, …, *n*, Eq. (3) can be rewritten as:

$$0 = \begin{bmatrix} \cos(\theta_{scfk}) \\ \sin(\theta_{scfk}) \end{bmatrix} \left(R_{scfk} i_{scfk} + \frac{d\lambda_{scfk}}{dt}\right) \quad (27)$$

Considering the transformation matrix of:

$$\begin{bmatrix} f_d^{scfk} \\ f_q^{scfk} \end{bmatrix} = \begin{bmatrix} \cos(\theta_{scfk}) \\ sin(\theta_{scfk}) \end{bmatrix} f_{scfk} \quad (28)$$

where f can be voltage, current, or flux linkage, the voltage of (27), after referring to the stator side can be written as:

$$0 = R_{scAk} \begin{bmatrix} I'_{scAk} \\ 0 \end{bmatrix} + \frac{d}{dt} k_{scAk}^2 \begin{bmatrix} \lambda'_{scAk} \\ 0 \end{bmatrix} \quad (29)$$

$$0 = R_{scBk} \begin{bmatrix} 0 \\ I'_{scBk} \end{bmatrix} + \frac{d}{dt} k_{scBk}^2 \begin{bmatrix} 0 \\ \lambda'_{scBk} \end{bmatrix} \quad (30)$$

where

$$\begin{bmatrix} \lambda'_{scAk} \\ 0 \end{bmatrix} = \begin{bmatrix} \lambda_d^m \\ 0 \end{bmatrix} \quad (31)$$

$$\begin{bmatrix} 0 \\ \lambda'_{scBk} \end{bmatrix} = \begin{bmatrix} 0 \\ \lambda_q^m \end{bmatrix} \quad (32)$$

Those equations can be used to draw an equivalent circuit for the resolver. In this regards, substituting (31) and (32), into (29) and (30), will result:

$$R_s \begin{bmatrix} I'_{scAk} \\ 0 \end{bmatrix} = -k_{scAk} \frac{d}{dt} \begin{bmatrix} \lambda_d^m \\ 0 \end{bmatrix} \quad (33)$$

$$R_s \begin{bmatrix} 0 \\ I'_{scBk} \end{bmatrix} = -k_{scBk} \frac{d}{dt} \begin{bmatrix} 0 \\ \lambda_q^m \end{bmatrix} \quad (34)$$

Furthermore, since the stator currents are negligible, the voltage drop on the stator windings' resistance and leakage inductance is almost zero. Therefore, substituting (25) into (22), will result in:

$$\frac{d}{dt} \begin{bmatrix} \lambda_d^m \\ \lambda_q^m \end{bmatrix} = \begin{bmatrix} v_d^s \\ v_q^s \end{bmatrix} \quad (34)$$

Then, substituting (35), into (33) and (34):

$$I'_{scAk} = \frac{-k_{scAk}}{R_s} v_d^s \quad (35)$$

$$I'_{scBk} = \frac{-k_{scBk}}{R_s} v_q^s \quad (36)$$

Then, the d-q equivalent circuit of the resolver under short circuit fault can be given as shown in Figs. 3-a, and 3-b. After simplifying the parallel branches, the simplified d-q circuit of Figs. 3-c, and 3-d is obtained.

The mentioned equations are employed in MATLAB/SIMULINK to analysis the performance of the sensor. The output voltages of SIMULINK are used to calculate the position error of the resolver. In this regard, Hilbert transform is used to obtain the envelope of the voltages [4]. Then, inverse tangent method is used for calculating the position. Comparing that position with the reference position leads to position error of the sensor. Fig. 4 shows the block diagram of the simulation.

The analog voltages of the health resolver obtained from the SIMULINK are presented in Fig. 5-a. After using Hilbert transform the envelope of the signals is obtained [4]. The envelope of the sine voltage versus that of cosine voltage is presented in Fig. 5-b. Then, harmonic content of the envelopes can be calculated. Total harmonic distortion (THD) of envelopes, maximum position error (MPE) and the average of absolute position error (AAPE) for the health resolver are 0.0531%, 0.2465°, and 0.0129°, respectively. It should be mentioned that the computation time required for one mechanical rotation of the rotor, using Intel® Core™i7-6500U CPU@2.50 GHz, is about one second. Therefore, the proposed analytical model can be employed in the on-line fault detection algorithms or design and optimization of the sensor.

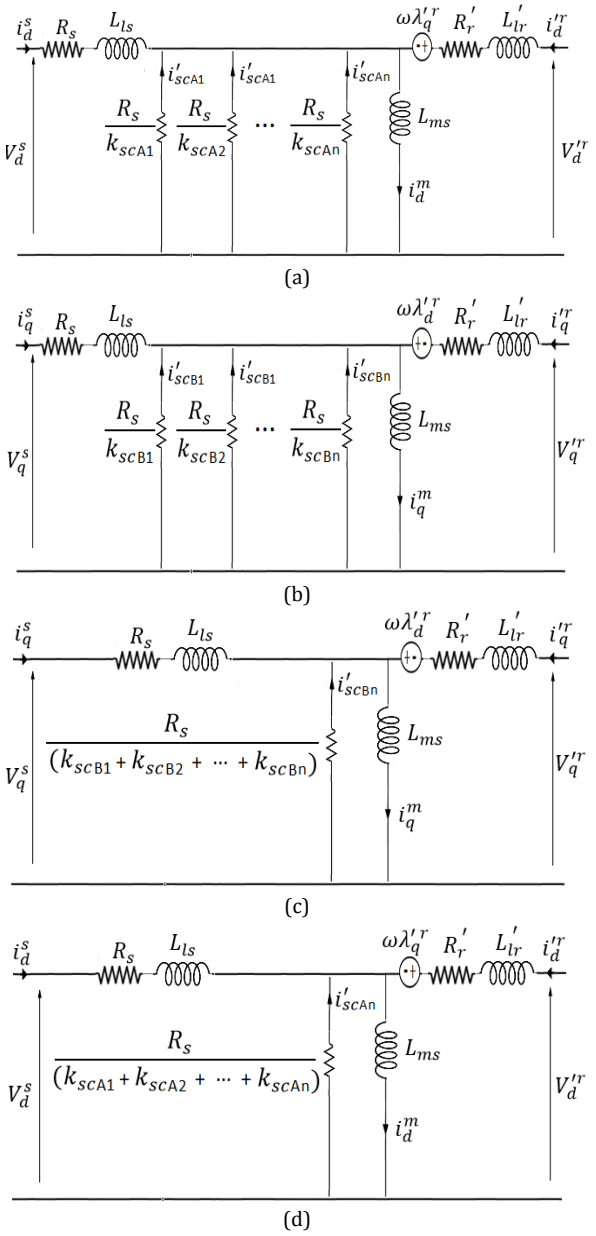

Figure 3: The equivalent circuit of the studied WR resolver under short circuit fault: (a) d-axis equivalent circuit, (b) q-axis equivalent circuit, (c) Simplified equivalent circuit of d-axis, and (d) Simplified equivalent circuit of q-axis.

The simulations are divided into two groups. In the first group, four independent short circuit faults are simulated. In the first simulation, called SC-1, the fault is considered on the cosine coil with maximum number of turns, where 1/16 of the turn numbers are shorted. In SC-2, 1/14 of the turns of cosine winding are shorted. In SC-3, and SC-4, 1/16 and 1/8 of the turn of sine winding are assumed to be short circuit, respectively. The second group that is referred to simultaneous faults consisted of three simulations. In SC-5, 1/16 of the turn numbers of both sine and cosine coils with maximum number of turns is considered.

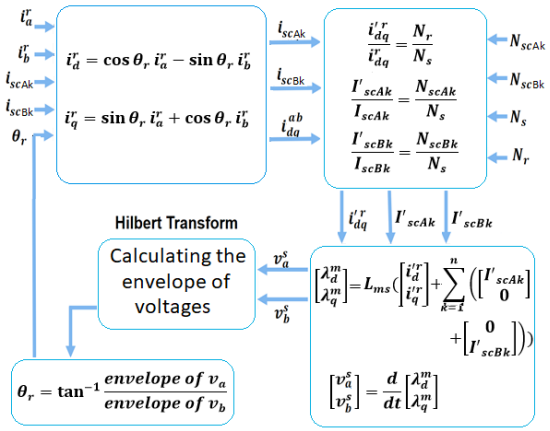

Figure 4: The block-diagram of the simulation.

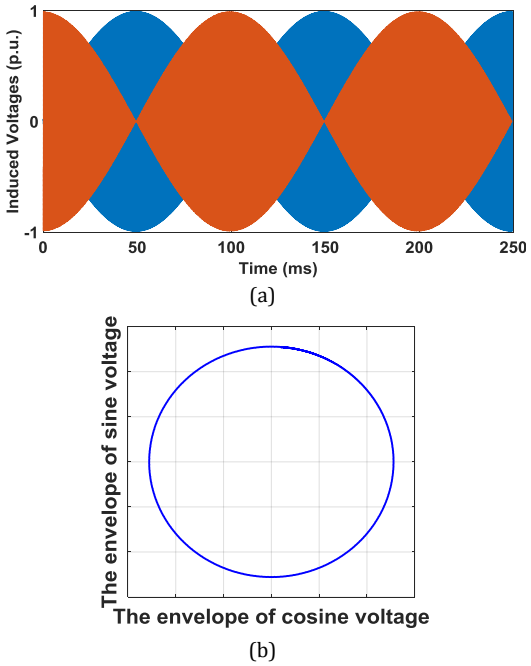

Figure 5: The results of the healthy sensor obtained from the proposed model: (a) Analogue voltages, (b) The envelope of sine voltage versus that of cosine voltage.

In the second simulation, SC-6, two short circuit faults (1/12 turn number on the coils with 130 turn number) on sine winding is considered. The last simulation is referred to two faults on the sine windings (1/16 turn short circuit on the cosine tooth of 150 turn number, and 1/8 turn on the coil with 75 turn number).

Harmonic contents of the sine and cosine voltages' envelope for the health resolver along with those for different independent fault conditions are presented in Figs. 6-a, and 6-b, respectively. Those results for the simultaneous faults are given in Figs. 6-c, and 6-d, respectively. It can be seen that the harmonic levels are increased under short circuit fault condition.

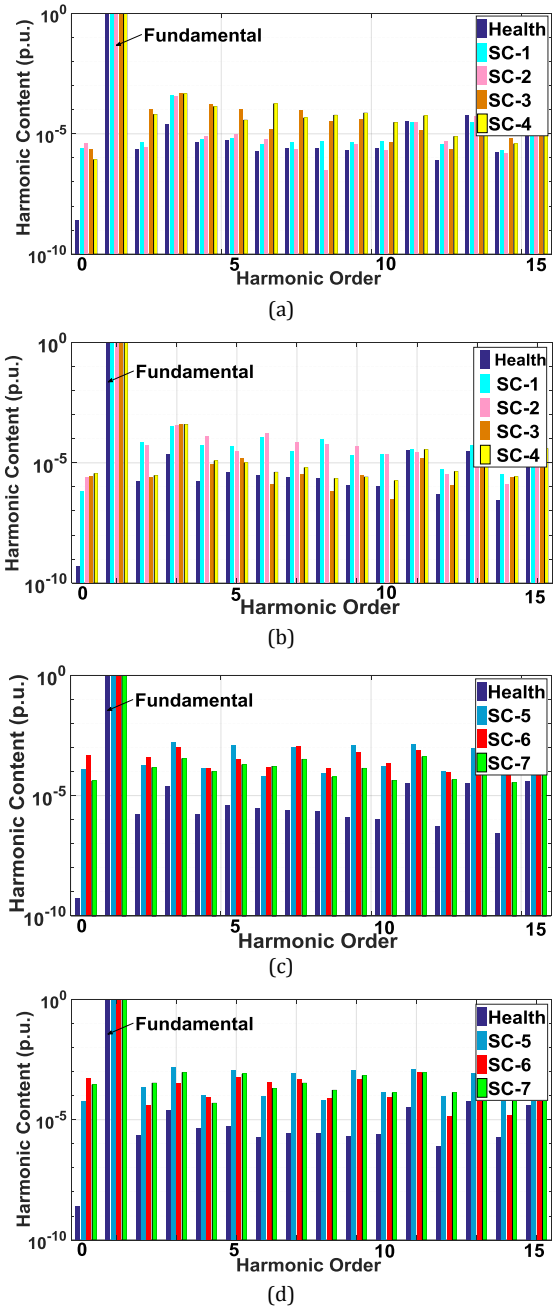

Figure 6: The harmonic content of the voltages' envelope: (a) for the sine voltage (independent faults), (b) for the cosine voltage (independent faults), (c) for the sine voltage (simultaneous faults), and (d) for the cosine voltage (simultaneous faults).

Figs. 7-a through 7-c show the variation of envelopes' THD, MPE, and AAPE under the different scenarios of short circuit faults using the proposed analytical model, respectively. Considering the results of THD and the AAPE, it seems that simultaneous short circuit faults have more destructive effect on the performance of the resolver. However, it should be mentioned that the most reliable index for performance evaluation of resolvers is AAPE. Because THD is not sensitive to the harmonic orders while position error is. Finally, it can be concluded that the performance of the sensor is significantly deteriorated under different short circuit faults. Therefore, it is required to diagnose the fault occurrence before its propagation to whole winding or undesirable performance of the drive system.

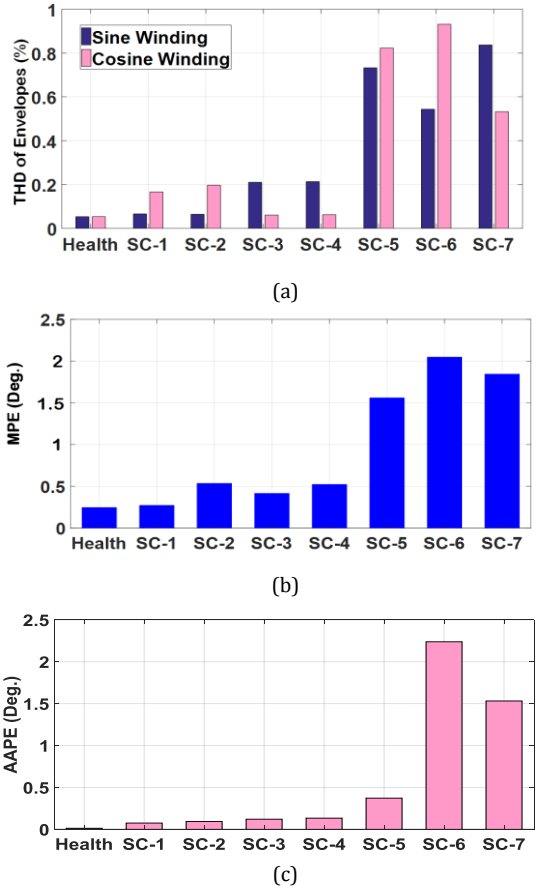

Figure 7: The performance of the studied resolver under different fault conditions: (a) THD of envelopes, (b) MPE, and (c) AAPE.

4. Experimental Evaluation

To evaluate the results of the proposed analytical model, an experimental test is carried out. The experimental test circuit is shown in Fig. 8-a. It can be seen that a DC motor is used to rotate the resolver with 300 rpm. The 4 kHz excitation voltage is built using a digitally synthesized function generator with the resolution of 0.1 Hz and the output signals are captured and saved using a digital oscilloscope. The output voltages are presented in Fig. 8-b. Those voltages are imported to the MATLAB to use Hilbert transform for calculating position error. Comparing the results of the experimental test with those of simulations indicates an acceptable agreement. However, the experimental position error is higher than that of simulation. To explain this difference, some points should be considered. The effect of rotary transformer is not considered in the simulations. So, for more agreement of results, it is required to model

the rotary transformer as well as the resolver. Furthermore, the non-linear behavior of the magnetizing core of the resolver is not taken into account. Although the operating point of resolvers is far from the saturation region [4], it may be stuck in the non-linear area of the beginning of the magnetizing curve. The other reason for difference between the results is using inaccurate parameters in d-q model. So, authors plan to conduct some more research on parameter identification of the resolver and improve the model by taking the RT and the non-linear magnetization curve of the ferromagnetic core into account.

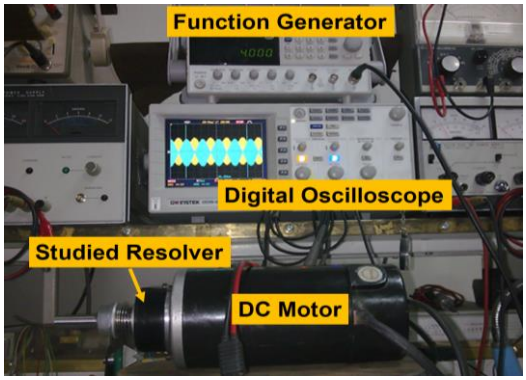

(a)

(b)

Figure 8: The experimental evaluation: (a) The test circuit, (b) The measured voltages.

5. Conclusion

Although the current of signal windings of the resolver is almost negligible, since their employed wire is very thin, there is high possibility of short circuit fault in signal windings. Therefore, in this paper a comprehensive mathematical model based on d-q axes theory was proposed to evaluate the performance of cylindrical, wound rotor resolvers under short circuit fault. Different amount/number of faults, even turn to turn short circuit faults, could be simulated using the proposed model, independently and simultaneously. Furthermore, the proposed model was fast enough to be integrated into an on-line fault detection algorithm. The simulations of the proposed model were done in MATLAB-SIMULINK and the Hilbert transform was used to decouple the excitation voltage. Then, the envelope of the AM voltages was used for calculating the position error. The results of the model were evaluated by comparing them with those of experimental measurement.

NOMENCLATURE

$\lambda^s_{ab}/v^s_{ab}/i^s_{ab}$	Flux linkages/voltages/currents of the stator
$\lambda^s_{dq}/v^s_{dq}/i^s_{dq}$	Flux linkages/voltages/currents of the stator in dq Reference frame
$\lambda^r_{ab}/v^r_{ab}/i^r_{ab}$	Flux linkages/voltages/currents of the rotor
$\lambda'^r_{dq}/v'^r_{dq}/i'^r_{dq}$	Flux linkages/voltages/currents of the rotor in dq Reference frame referred to the stator side
I_{scAk}/I_{scBj}	The current of kth short circuit on phase A/B
I'_{scAk}/I'_{scBk}	The current of kth short circuit referred to the stator Side on phase A/B
$\lambda'_{scAk}/\lambda'_{scBk}$	The flux linkages of kth short circuit referred to the stator side on phase A/B
$\lambda^{ls}_{dq}/\lambda'^{lr}_{dq}$	Leakage flux of the stator/rotor winding
$[T_{dq}]$	d-q transformation matrix
θ_r	Rotor position
R_s/R_r	Stator/rotor resistance
R_{scAk}/R_{scBk}	kth short circuit resistance on phase A/B
L^{ss}_{ab}	Matrices of stator-to-stator inductances
L^{rr}_{ab}	Matrices of rotor-to-rotor inductances
L^{sr}_{ab}	Matrices of mutual inductances stator-to-rotor
$L^{scAkscAj}$	Matrices of inductances kth short circuit in phase A to jth short circuit in phase A
$L^{scBkscBj}$	Matrices of inductances kth short circuit in phase B to jth short circuit in phase B
L^{scAkr}/L^{scBkr}	Matrices of mutual inductances kth short circuit in phase A/B to the rotor
L_{ms}/L_{mr}	The mutual inductance between the stator/rotor windings
L_{ls}/L_{lr}	The leakage inductance of stator/rotor winding
L_{sr}	The peak value of the mutual inductance stator-to-rotor
L_{scAkr}/L_{scBkr}	The peak value of mutual inductances of the kth short circuit in phase A/B to rotor
L_{scAks}/L_{scBks}	Value of the kth short circuit in phase A/B to stator mutual inductances
N_s/N_r	Stator/rotor turn numbers
N_{scBk}/N_{scBk}	kth short circuit on phase A/B turn numbers

Acknowledgement

This work is partially supported by grant from Niroo research institute and the research office of Sharif University of Technology (SUT).

References

[1] P. Vahedi and B. Ganji, "A switched reluctance motor with lower temperature rise and acoustic noise," *Journal of Electrical and Computer Engineering Innovations*, vol. 6, no. 1, pp. 43-52, 2018.

[2] M. Ahmadi Darmani and H. Hooshyar, "Optimal design of axial flux permanent magnet synchronous motor for electric vehicle applications using GA and FEM," *Journal of Electrical and Computer Engineering Innovations*, vol. 3, no. 2, pp. 89-97, 2015.

[3] R. Alipour-Sarabi, Z. Nasiri-Gheidari, F. Tootoonchian, and H. Oraee, "Improved winding proposal for wound rotor resolver using genetic algorithm and winding function approach," *IEEE Trans. Ind. Electron.*, vol. 66, no. 2, pp. 1325-1334, Feb. 2019.

[4] H. Saneie, R. Alipour-Sarabi, Z. Nasiri-Gheidari, and F. Tootoonchian, "Challenges of finite element analysis of resolvers," *IEEE Trans. Energy Convers*., vol. 34, no. 2, pp. 973-983, 2019.

[5] Z. Nasiri-Gheidari, "Design, analysis, and prototyping of a new wound-rotor axial flux brushless resolver," *IEEE Trans. Energy Convers.*, vol. 32, no. 1, pp. 276 - 283, 2017.

[6] F. Abolqasemi-Kharanaq, R. Alipour-Sarabi, Z. Nasiri-Gheidari, and F. Tootoonchian, "Magnetic equivalent circuit model for wound rotor resolver without rotary transformer's core," *IEEE Sensors J*., vol. 18, no. 21, pp. 8693-8700, Nov. 2018.

[7] A. Farhadi-Beiranvand, R. Alipour-Sarabi, Z. Nasiri-Gheidari, and F. Tootoonchian, "Selection of excitation signal waveform for improved performance of wound rotor resolver," presented at The Power Electronics, Drive Systems and Technologies Conference (PEDSTC), Shiraz, Iran, 2018

[8] H. Saneie, Z. Nasiri-Gheidari, and F. Tootoonchian, "Design-oriented modelling of axial-flux variable-reluctance resolver based on magnetic equivalent circuits and schwarz–christoffel mapping," *IEEE Trans. Ind. Electron*., vol. 65, no. 5, pp. 422-4330, 2018.

[9] X. Ge, Z. Q. Zhu, R. Ren, and J. T. Chen, "Analysis of windings in variable reluctance resolver," *IEEE Trans. Magn*., vol. 51, no. 5, pp. 1-10, May 2015.

[10] A Daniar, Z Nasiri-Gheidari, and F Tootoonchian, "Performance analysis of linear variable reluctance resolvers based on improved winding function approach," *IEEE Trans. Energy Conversion*, vol. 33, no. 3, pp. 1422-1430, Sep. 2018.

[11] H. Saneie, Z. Nasiri-Gheidari, and F. Tootoonchian, "Accuracy improvement in variable reluctance resolvers," *IEEE Trans. Energy Convers*., vol. 34, no. 3, pp. 1563-1571, 2019.

[12] Z. Nasiri-Gheidari, R. Alipour-Sarabi, F. Tootoonchian, and F. Zare, "Performance evaluation of disk type variable reluctance resolvers," *IEEE Sensors J*., vol. 17, no. 13, pp. 4037-4045, July 2017.

[13] M. Bahari and Z. Nasiri-Gheidari, "Longitudinal end effect in variable area linear resolver and its compensating methods," in *Proc. 2018 Iranian Conference on Electrical Engineering (ICEE)*, pp. 1316-1321, 2018.

[14] M. Bahari, R. Alipour-Sarabi, Z. Nasiri-Gheidari, and F. Tootoonchian, "Proposal of winding function model for geometrical optimization of linear sinusoidal area resolver," *IEEE Sensors J.*, vol. 19, no. 14, pp. 5506-5513, 2019.

[15] F. Tootoonchian, "Proposal of a new affordable 2-pole resolver and comparing its performance with conventional wound-rotor and VR resolvers," *IEEE Sensors J*., vol. 18, no. 13, pp. 5284-5290, 2018.

[16] F. Tootoonchian, "Effect of damper winding on accuracy of wound-rotor resolver under static-, dynamic and mixed-eccentricities," *IET Electric Power Applications*, vol. 12, no. 6, pp. 845-851, 2018.

[17] H. Saneie, Z. Nasiri-Gheidari, and F. Tootoonchian, "The influence of winding's pole pairs on position error of linear resolvers," in *Proc. 25th Iranian Conference on Electrical Engineering (ICEE),* pp. 949-954, 2017.

[18] A. Daniar and Z. Nasiri-Gheidari, "The influence of different configurations on position error of linear variable reluctance resolvers," in *Proc. 25th Iranian Conference on Electrical Engineering (ICEE),* pp. 955-960, 2017.

[19] P. Naderi and A. Shiri, "Rotor/stator inter-turn short circuit fault detection for saturable wound-rotor induction machine by modified magnetic equivalent circuit approach," *IEEE Trans. Magnetic*, vol. 54, no. 11, 2017.

[20] K. C. Kim, "Analysis on the charateristics of variable reluctance resolver considering uneven magnetic fields," *IEEE Trans. Magn*., vol. 49, no. 7, pp. 1-4, July 2013.

[21] F. Tootoonchian and F. Zare, "Performance analysis of disk type variable reluctance resolver under mechanical and electrical faults," *Iran. J. Electr. Electron. Eng*., vol. 14, no. 3, pp. 299-307, 2018

[22] F. Zare, Z. Nasiri-Gheidari, and F. Tootoonchian, "The effect of winding arrangements on measurement accuracy of sinusoidal rotor resolver under fault conditions," *Measurement*, vol. 131, pp. 162-172, 2019.

[23] H. Lasjerdi, Z. Nasiri-Gheidari, and F. Tootoonchian, "Proposal of an analytical model for performance evaluation of WR-resolvers under short circuit fault," presented at the 27th Iranian Conference on Electrical Engineering (ICEE2019), Yazd, Iran, 2019.

BIOGRAPHIES

Hamed Lasjerdi has received his B.Sc. degree in Electrical Engineering from Iran University of Science and Technology, Tehran, Iran in 2017 and he received the Master degree in Electrical Power Engineering from Sharif University of Technology, Tehran, Iran, in 2019, graduating with First Class Honors in both of them. He is currently working toward the Ph.D. degree in Sharif University of Technology, Tehran, Iran. His research interests are in condition monitoring and diagnostics, and analysis of electromagnetic sensors.

Zahra Nasiri-Gheidari received the B.Sc. degree from Iran University of Science and Technology, Tehran, Iran, in 2004, and the M.Sc. and Ph.D. degrees from University of Tehran, Tehran, in 2006 and 2012, respectively, all in Electrical Engineering. She is currently an Associate Professor with the Department of Electrical Engineering, Sharif University of Technology, Tehran, Iran. Her research interests include design, optimization, and performance analysis of electrical machines and electromagnetic sensors.

Farid Tootoonchian received the B.Sc. and M.Sc. degrees in Electrical Engineering from Iran University of Science and Technology, Tehran, Iran, in 2000 and 2007, respectively, and the Ph.D. degree from K. N. Toosi University of Technology, Tehran, in 2012. He is currently an Assistant Professor with the Department of Electrical Engineering, Iran University of Science and Technology, Tehran, Iran. His research interests include design, optimization, finite-element analysis, and prototyping of ultrahigh-speed electrical machines and ultrahigh-precision electromagnetic sensors.

How to cite this paper:
H. Lasjerdi, Z. Nasiri-Gheidari, and F. Tootoonchian, "A comprehensive mathematical model for analysis of WR-resolvers under stator short circuit fault," *Journal of Electrical and Computer Engineering Innovations*, vol. 7, no. 1, pp. 11-18, 2019.
DOI: 10.22061/JECEI.2019.5558.237
URL: http://jecei.sru.ac.ir/article_1137.html